Lossless and loss-induced topological transitions of isofrequency surfaces in a biaxial gyroelectromagnetic medium

Volodymyr I. Fesenko[1,2] and Vladimir R. Tuz[1,2,*]

[1]*International Center of Future Science, State Key Laboratory of Integrated Optoelectronics, College of Electronic Science and Engineering, Jilin University, 2699 Qianjin Street, Changchun 130012, China*

[2]*Institute of Radio Astronomy of National Academy of Sciences of Ukraine, 4, Mystetstv Street, Kharkiv 61002, Ukraine*

(Received 19 November 2018; revised manuscript received 16 January 2019; published 5 March 2019)

Topological transitions of isofrequency surfaces are studied in the long-wavelength approximation for a biaxial gyroelectromagnetic medium influenced by an external static magnetic field. For the lossless case, the topological transitions from a closed ellipsoid to open type-I and type-II hyperboloids as well as a bihyperboloid are demonstrated. Conditions for critical points where the topological transitions occur are found out. It is revealed that material losses in the constituents of the composite medium strongly influence the dispersion of the extraordinary waves. In particular, the loss-induced topological transitions take place for these waves. It is shown that the loss-induced topological transitions from a type-I hyperboloid to a bihyperboloid appear in the frequency band where the real part of at least one principal component of the anisotropic constitutive parameter (permittivity or permeability tensor) is close to zero, whereas its imaginary part is high.

DOI: 10.1103/PhysRevB.99.094404

I. INTRODUCTION

During the past decade hyperbolic metamaterials have been a subject of intense study due to their specific dispersion features that are unattainable in conventional media [1]. At present they are realized experimentally in the microwave, terahertz, and optical ranges and demonstrate several unusual properties, including negative refraction [2], strong enhancement of spontaneous emission [3], broadband infinite density of states [4], subwavelength imaging [5], focusing [6], and signal routing [7].

Hyperbolic dispersion appears in *extremely* anisotropic media (also known as *indefinite* media [8]). In such media, at least one constitutive parameter is necessarily a tensor quantity $\hat{\eta} = [\eta_{xx}, 0, 0; 0, \eta_{yy}, 0; 0, 0, \eta_{zz}]$ (here η is either permeability μ or permittivity ε), whereas one of the principal components of the tensor $\hat{\eta}$ differs in sign from other principal components. A medium is called a hyperbolic uniaxial crystal or a hyperbolic biaxial crystal when the tensor's diagonal components satisfy one of the following conditions: $\eta_{xx} < 0 < \eta_{yy} = \eta_{zz}$ and $\eta_{xx} < 0 < \eta_{yy} < \eta_{zz}$. In the indefinite media, the topological transitions of isofrequency surfaces appear when the real part of a particular component of the permittivity or permeability tensor changes sign.

Typically, hyperbolic dispersion is observed in nonmagnetic metamaterials characterized by an indefinite permittivity tensor and scalar permeability ($\mu_{xx} = \mu_{yy} = \mu_{zz} = 1$). Since the negative value of permittivity is an ordinary property for metals under the plasmonic conditions, the design of hyperbolic metamaterials usually incorporates metallic components. In such a design the metamaterials are made either in the form of a superlattice which combines metallic and dielectric layers [9–11] or a lattice of conducting wires embedded into a dielectric host [12–15]. Regardless of design, the overall structure is considered as an effective medium under the long-wavelength approximation, which imposes limitation on the size of structural components [16]. Alternatively, hyperbolic metamaterials can be implemented utilizing the indefinite permeability tensor. This feature emerges in a narrow frequency band for metamaterials composed of metallic split-ring resonators [17].

The hyperbolic dispersion exists also in natural media featuring gyroelectric (e.g., plasma or semiconductor) or gyromagnetic (e.g., ferrite) properties under the influence of an external static magnetic field. Under saturated magnetization such media become extremely anisotropic in a specific frequency band due to clear-cut plasma or ferromagnetic resonance. This leads to the appearance of a hyperbolic form of isofrequency surfaces related to particular waves (in optics of anisotropic media [18–21], the waves whose propagation is influenced by the external static magnetic field are denoted as *extraordinary* waves, otherwise they are called *ordinary* waves). In the general case of a biaxial gyroelectric or gyromagnetic medium there are topological transitions of isofrequency surfaces for the extraordinary waves from a closed ellipsoid ($0 < \eta_{xx} < \eta_{yy} < \eta_{zz}$) to open a type-I ($\eta_{xx} < 0 < \eta_{yy} < \eta_{zz}$) asymmetric hyperboloid or a type-II ($\eta_{xx} < \eta_{yy} < 0 < \eta_{zz}$) asymmetric hyperboloid [13,22]. For ordinary waves, the dispersion properties are characterized by isofrequency surfaces in the form of a closed ellipsoid.

The topological transitions of isofrequency surfaces are usually studied separately for gyroelectric [19] or gyromagnetic media [20,21]. However, it is demonstrated [23–32] that the semiconductor and magnetic materials combined together into a unified gyroelectromagnetic structure (superlattice) with tensorlike forms of both permittivity and permeability gives unprecedented flexibly for manipulating the dispersion

*tvr@jlu.edu.cn; tvr@rian.kharkov.ua

of both surface and bulk waves. In particular, in such a superlattice the topological transitions from a closed ellipsoid to open type-I and type-II hyperboloids as well as a bihyperboloid are observed for the extraordinary waves [33]. The bihyperboloid is a form of isofrequency surface, which was discovered recently and arises from simultaneous tuning of superlattice geometry and external static magnetic field.

Typically, in order to simplify simulations and description of obtained results, actual losses in constituents of a metamaterial are totally ignored assuming $\hat{\varepsilon}$ and $\hat{\mu}$ to be real-valued tensors. In fact, such an approximation is good for conventional isotropic and anisotropic media ($\varepsilon_{ii} \geqslant 1,\ \mu_{ii} \geqslant 1,\ \varepsilon_{ij} = \mu_{ij} = 0,\ i \neq j,\ i, j = x, y, z$) in which intrinsic losses are only responsible for attenuation of propagated electromagnetic wave [34,35].

However, recently it has been reported [36] that the presence of intrinsic losses in the ε-near-zero medium can play a positive role in the wave propagation. For instance, it can enhance transmission and collimate the field inside the medium. Moreover, it was experimentally observed [37,38] that in the μ-near-zero metamaterial constructed from two-dimensional transmission lines with lumped elements (resistors), a topological transition of isofrequency surfaces from a closed ellipsoid to an open type-I hyperboloid appears. This topological transition is related to variation of the imaginary part of permeability for fixed values of both the real part of permeability and the frequency. It is called *loss-induced* topological transition, and it is qualitatively different from transitions associated with the sign change in the real part of permittivity or permeability. Several wave effects, namely, collimation and field enhancement during the wave propagation, were observed experimentally in the transmission-line-based metamaterial [37] supporting loss-induced transitions. The loss-induced transitions were also found in the two-dimensional transmission line metamaterials with an arbitrary positive real part of permeability [38] and in a one-dimensional periodic structure composed of graphene sheets deposited on dielectric layers [39].

In the present paper our main goal is to reveal characteristics of the topological transitions of isofrequency surfaces for the waves propagating through a gyroelectromagnetic structure. The existence of such transitions is expected since in the frequency bands near the plasma or ferromagnetic resonance, the gyroelectromagnetic structure behaves as an ε-near-zero or μ-near-zero medium. In these frequency bands, the intrinsic losses in constitutive materials are usually high and can lead to the appearance of loss-induced topological transitions which are of our particular interest.

The rest of the paper is organized as follows: In Sec. II we formulate and solve the problem related to the bulk waves propagating through a biaxial gyroelectromagnetic medium. Then in Sec. III, we discuss the topological transitions of isofrequency surfaces in the idealized lossless biaxial gyroelectromagnetic medium and reveal the specific conditions of their occurrence. In Sec. IV we extend the theory to account for intrinsic losses of actual materials incorporated into the structure and show the characteristics of loss-induced topological transitions, which appear under certain geometrical and material parameters of the superlattice. Finally, in Sec. V we summarize the paper. The expressions for tensors describing constitutive properties of ferrite and semiconductor materials are given in the Appendix for clarity.

II. DISPERSION RELATION FOR BULK WAVES

We study topological transitions of isofrequency surfaces related to a periodic (along the y axis) multilayered structure (superlattice) of magnetic (ferrite) and semiconductor layers with thicknesses d_m and d_s, respectively. The structure is infinitely extended along the transverse directions [Fig. 1(a)]. The period of the structure is $d = d_m + d_s$. All layers of the superlattice are magnetized uniformly by an external static magnetic-field $\vec{M}$ directed along the z axis transversely to the structure periodicity. Under the influence of such a magnetization, individual magnetic and semiconductor layers of the superlattice are characterized by the combination of tensor constitutive parameters $\hat{\mu}_m$, ε_m and μ_s, $\hat{\varepsilon}_s$. For clarity, the tensors $\hat{\mu}_m$ and $\hat{\varepsilon}_s$ and their components as functions of frequency are given in Fig. 1(b) (see also the expressions for components of the tensors $\hat{\mu}_m$ and $\hat{\varepsilon}_s$ in the Appendix).

We suppose that all characteristic dimensions of the superlattice, namely, its period and the thicknesses of the constitutive layers, satisfy the long-wavelength limit, that is, $d_m \ll \lambda,\ d_s \ll \lambda,\ d \ll \lambda$, where λ is the wavelength inside the medium. In this case, the standard homogenization procedure of the effective medium theory [40] is applied to derive averaged expressions for effective parameters of the superlattice. The results of the homogenization procedure are checked against those of the rigorous transfer-matrix technique [41,42], and a good correlation is found for the chosen structure parameters and frequency. Therefore, the superlattice is closely approximated by an infinite bigyrotropic medium [Fig. 1(c)], which is characterized by relative effective permeability $\hat{\mu}_{\text{eff}}$ and relative effective permittivity $\hat{\varepsilon}_{\text{eff}}$, each in the form of the second-rank tensors (all details on the homogenization procedure are omitted here and can be found in Ref. [43]). For the homogenized medium all principal components of permittivity and permeability have different values, namely, $\varepsilon_{xx} \neq \varepsilon_{yy} \neq \varepsilon_{zz}$ and $\mu_{xx} \neq \mu_{yy} \neq \mu_{zz}$, and the nondiagonal element corresponds to a biaxial bigyrotropic ($\varepsilon_{xy} = -\varepsilon_{yx} \neq 0$ and $\mu_{xy} = -\mu_{yx} \neq 0$) crystal. In this crystal one of the optical axes is directed along the structure periodicity (the y axis), whereas the second one coincides with the direction of the external magnetic field (the z axis). It should be noted, that the anisotropy of the structure is strongly dependent on both the ratio between thicknesses of the magnetic and semiconductor layers and the magnetic-field strength. The corresponding dispersion characteristics of the components of relative effective permeability $\hat{\mu}_{\text{eff}}$ and relative effective permittivity $\hat{\varepsilon}_{\text{eff}}$ are given in Fig. 1(d) for reference.

In the following discussion we consider a plane uniform electromagnetic wave with angular frequency ω and wave-vector $\vec{k}$ which propagates in a biaxial gyroelectromagnetic medium along an arbitrary direction as shown in Fig. 1(c). The electric- ($\vec{E}$) and magnetic- ($\vec{H}$) field vectors can be expressed as

$$\vec{E}(\vec{H}) = \vec{E}_0(\vec{H}_0)\exp[i(k_x x + k_y y + k_z z - \omega t)], \qquad (1)$$

where $k_x = k\sin\theta\cos\varphi$, $k_y = k\sin\theta\sin\varphi$, and $k_z = k\cos\theta$ are the Cartesian coordinates of the wave-vector $\vec{k}$.

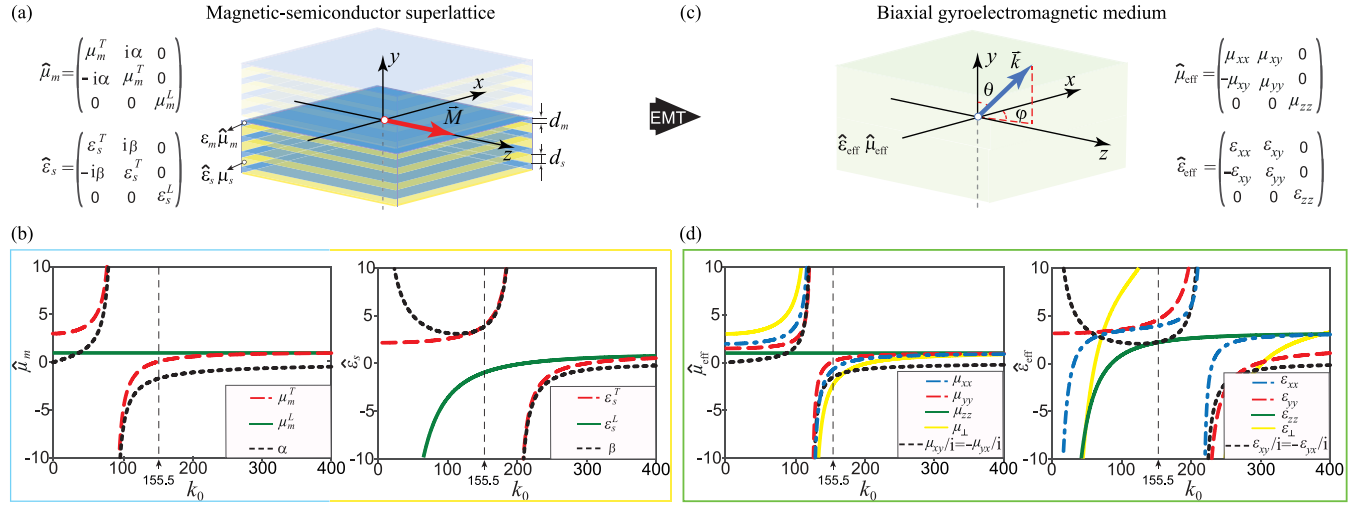

FIG. 1. The problem sketch related to: (a) a magnetic-semiconductor superlattice influenced by an external static magnetic-field $\vec{M}$; (c) resulting homogenized medium (biaxial gyroelectromagnetic medium). Dispersion curves (real parts) of the tensor components of: (b) permeability $\hat{\mu}_m$ and permittivity $\hat{\varepsilon}_s$ of magnetic and semiconductor layers, respectively; (d) relative effective permeability $\hat{\mu}_{\text{eff}}$ and relative effective permittivity $\hat{\varepsilon}_{\text{eff}}$ of the homogenized medium with $\delta_m = \delta_s = 0.5$. For the magnetic layers, under saturation magnetization of 2930 G, the parameters are as follows: $\omega_0/2\pi = 4.2$ GHz, $\omega_m/2\pi = 8.2$ GHz, $b = 0$, $\varepsilon_m = 5.5$. For the semiconductor layers, the parameters are as follows: $\omega_p/2\pi = 10.5$ GHz, $\omega_c/2\pi = 9.5$ GHz, $\nu/2\pi = 0$ GHz, $\varepsilon_l = 1.0$, $\mu_s = 1.0$.

From Maxwell's equations, the dispersion equation, which relates $\omega = k_0 c$ to $\vec{k} = \{k_x, k_y, k_z\}$ and describes propagation of electromagnetic waves through an unbounded gyroelectromagnetic medium, can be written as follows (the required mathematical manipulations are omitted here and can be found in Refs. [20,34]):

$$
\begin{aligned}
&(\varepsilon_{zz}\mu_{zz})^{-1}\{k_x^4\varepsilon_{xx}\mu_{xx} + k_y^4\varepsilon_{yy}\mu_{yy} + k_z^4\varepsilon_{zz}\mu_{zz} + k_x^2k_y^2 \\
&\times(\varepsilon_{xx}\mu_{yy} + \varepsilon_{yy}\mu_{xx}) + k_x^2k_z^2(\varepsilon_{xx}\mu_{zz} + \varepsilon_{zz}\mu_{xx}) + k_y^2k_z^2 \\
&\times(\varepsilon_{yy}\mu_{zz} + \varepsilon_{zz}\mu_{yy}) - k_0^2[k_x^2(\varepsilon_{xx}\varepsilon_{zz}\mu_\perp + \mu_{xx}\mu_{zz}\varepsilon_\perp) \\
&+ k_y^2(\varepsilon_{yy}\varepsilon_{zz}\mu_\perp + \mu_{yy}\mu_{zz}\varepsilon_\perp) + k_z^2\varepsilon_{zz}\mu_{zz}(\varepsilon_{xx}\mu_{yy} \\
&+ \varepsilon_{yy}\mu_{xx} - 2\varepsilon_{xy}\mu_{xy})]\} + k_0^4\varepsilon_\perp\mu_\perp = 0, \qquad (2)
\end{aligned}
$$

where $\varepsilon_\perp = \varepsilon_{xx}\varepsilon_{yy} + \varepsilon_{xy}^2$ and $\mu_\perp = \mu_{xx}\mu_{yy} + \mu_{xy}^2$ are two generalized transverse effective constitutive parameters of homogenized medium. For clarity, the dispersion curves of parameters $\varepsilon_\perp$ and $\mu_\perp$ are shown in Fig. 1(d) by solid yellow lines.

At a constant frequency biquadratic dispersion Eq. (2) is known as Fresnel's equation for wave normals [34] and describes a fourth-order (*quartic*) surface in the k_x, k_y, and k_z coordinate space (in the k space). Such a surface is called an isofrequency surface (or, alternatively, the Fresnel wave surface or surface of wave vectors). In normalized terms of $\kappa = k/k_0$, Eq. (2) can be written as [33]

$$A\kappa^4 + B\kappa^2 + C = 0, \qquad (3)$$

whose solution is

$$\kappa^2 = (B \pm \sqrt{B^2 - 4AC})/2A. \qquad (4)$$

Here, $A = (\varepsilon_{zz}\mu_{zz})^{-1}(\overline{\varepsilon}\sin^2\theta + \varepsilon_{zz}\cos^2\theta)(\overline{\mu}\sin^2\theta + \mu_{zz}\cos^2\theta)$, $B = -[(\varepsilon_{xx}\mu_{yy} + \mu_{xx}\varepsilon_{yy} - 2\varepsilon_{xy}\mu_{xy})\cos^2\theta + (\varepsilon_{zz}\mu_{zz})^{-1}(\varepsilon_\perp\overline{\mu}\mu_{zz} + \mu_\perp\overline{\varepsilon}\varepsilon_{zz})\sin^2\theta]$, $C = \varepsilon_\perp\mu_\perp$, $\overline{\varepsilon} = \varepsilon_{xx}\cos^2\varphi + \varepsilon_{yy}\sin^2\varphi$, and $\overline{\mu} = \mu_{xx}\cos^2\varphi + \mu_{yy}\sin^2\varphi$.

We should note, that both Eqs. (2) and (3) represent in different forms the dispersion equation for bulk waves propagating in an unbounded biaxial gyroelectromagnetic medium. The solution of this dispersion equation gives us the possibility to reveal characteristics of the electromagnetic field inside the structure for the given set of geometrical and material parameters of the superlattice, so the *direct* problem is formulated and solved here. Recently an elegant solution of the corresponding *inverse* problem has been reported [44].

For a lossless medium, the isofrequency surfaces are related to the purely real roots of Eq. (3). In the general case, Eq. (3) yields two real roots κ_1 and κ_2, and two isofrequency surfaces exist for any frequency. In accordance with accepted notation [35], one of such roots [with upper sign + in Eq. (4)] is related to the *ordinary* waves, whereas another one [with lower sign − in Eq. (4)] is related to the *extraordinary* waves. When one of the roots κ_1 or κ_2 is a purely imaginary quantity and corresponds to propagation of an evanescent wave, only one isofrequency surface exists at the given frequency.

Furthermore, in a lossy medium, the components of effective constitutive tensors $\hat{\varepsilon}_{\text{eff}}$ and $\hat{\mu}_{\text{eff}}$ are complex, that is, $\varepsilon_{ij} = \varepsilon'_{ij} + i\varepsilon''_{ij}$ and $\mu_{ij} = \mu'_{ij} + i\mu''_{ij}$ for $i, j = x, y, z$. In this case, all four roots of Eq. (3) are complex quantities ($\kappa_i = \kappa'_i + i\kappa''_i$, $i = 1$–4) and describe propagation of complex waves. Their amplitudes may either decay or grow exponentially during the wave propagation. Complex waves with exponentially decaying amplitude ($\kappa''_i > 0$) correspond to the *proper* waves [45,46], otherwise ($\kappa''_i < 0$) they are related to the *improper* waves, which are nonphysical solutions for a passive medium.

III. LOSSLESS TOPOLOGICAL TRANSITIONS

Our objective here is to study the topological transitions of isofrequency surfaces related to the waves propagating through an idealized lossless gyroelectromagnetic medium. Although we neglect losses, all other parameters of the given

superlattice are set equal to typical values for actual materials. In particular, in this paper we follow the results of Ref. [24] and study the superlattice made of barium cobalt (e.g., $Ba_3Co_2Fe_{24}O_{41}$) [47] and doped-silicon [48] layers. This choice explained by the fact that under the influence of an external magnetic field the characteristic resonant frequencies for these materials are closely spaced [see Fig. 1(b)]. All geometrical and material parameters of the magnetized superlattice are summarized in the caption of Fig. 1. For all our subsequent calculations the frequency parameter is assumed to be $k_0 = 155.5\ \mathrm{m}^{-1}$ ($f \approx 7.4$ GHz).

In the superlattice under study, the externally applied static magnetic field can essentially change the dispersion characteristics of the medium since it simultaneously influences both permeability and permittivity of magnetic and semiconductor layers, respectively. The dispersion characteristics depend also on the direction of structure periodicity and ratio between filling factors of the magnetic and semiconductor constituents of the superlattice (we introduce corresponding filling factors as dimensionless parameters written in the form $\delta_m = d_m/d$, $\delta_s = d_s/d$, and $\delta_m + \delta_s = 1$). Nevertheless, it is revealed [33] that the topological transitions of isofrequency surfaces appear due to the changes in the principal values of tensors of relative effective permeability $\hat{\mu}_{\mathrm{eff}}$ and relative effective permittivity $\hat{\varepsilon}_{\mathrm{eff}}$. At a constant external magnetic-field strength, these parameters are functions of the superlattice filling factors only.

For the given parameters of the superlattice, the following relations between the values of principal components of tensors $\hat{\mu}_{\mathrm{eff}}$ and $\hat{\varepsilon}_{\mathrm{eff}}$ hold: $\mu_{zz} > \mu_{yy} > \mu_{xx}$ and $\varepsilon_{yy} > \varepsilon_{xx} > \varepsilon_{zz}$. The principal values ε_{yy}, ε_{xx}, and μ_{yy} are always positive quantities, and $\mu_{zz} = 1$ regardless of the value of δ_m ($\delta_m \in [0.0, 1.0]$). Moreover, several representative regions can be distinguished by different combinations of positive and negative values of principal components ε_{zz} and μ_{xx}, which depend on δ_m [corresponding regions are denoted by Roman numerals "I–IV" and depicted in different colors in Fig. 2(a)]. They are as follows: (Region I) $\delta_m \in [0.0, 0.05)$, where $\varepsilon_{zz} < 0$ and $\mu_{xx} > 0$; (Region II) $\delta_m \in [0.05, 0.16)$, where $\varepsilon_{zz} < 0$ and $\mu_{xx} < 0$; (Region III) $\delta_m \in [0.16, 0.95)$, where $\varepsilon_{zz} > 0$ and $\mu_{xx} < 0$; (Region IV) $\delta_m \in [0.95, 1.0]$, where $\varepsilon_{zz} > 0$ and $\mu_{xx} > 0$.

These different combinations of values of ε_{zz} and μ_{xx} correspond to distinct forms of isofrequency surfaces arising from certain topological transitions. These transitions appear when either value ε_{zz} or μ_{xx} goes to zero at some δ_m. These values separate topologically distinct sets of solutions of Eq. (3) [we depict the transition points in Fig. 2(a) by stars]. Therefore, we plot the corresponding set of isofrequency surfaces in Figs. 2(b)–2(h) for Regions I–IV, respectively, where in the k space each component of the wave vector is normalized by k_0. In the plotted data, green and blue surfaces correspond to the ordinary and extraordinary waves, respectively.

In Region I all principal components of $\hat{\mu}_{\mathrm{eff}}$ are positive and $|\mu_{xy}^2| < |\mu_{xx}\mu_{yy}|$, whereas the component ε_{zz} of $\hat{\varepsilon}_{\mathrm{eff}}$ is negative. As is typical for the hyperbolic metamaterial [11], the isofrequency surfaces arise in the forms of an ellipsoid for the ordinary waves and a twofold type-I uniaxial hyperboloid for the extraordinary waves [Fig. 2(b)]. A distinctive feature

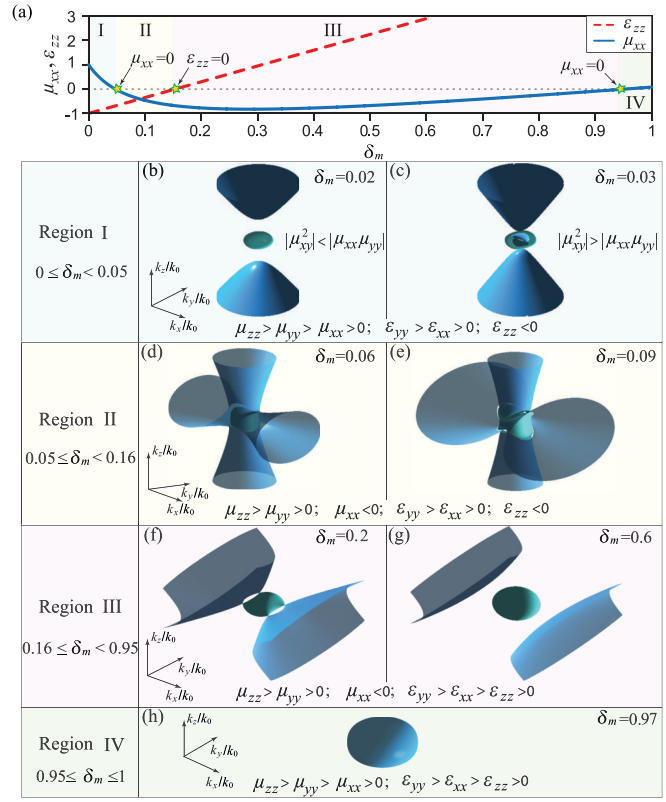

FIG. 2. (a) The change in the values of principal components μ_{xx} and ε_{zz} as the parameter δ_m varies at a fixed frequency. (b)–(h) The forms of isofrequency surfaces related to waves propagating through a lossless superlattice for different values of the parameter δ_m. Green and blue surfaces correspond to behaviors of ordinary and extraordinary waves, respectively.

of the hyperboloid is its slight compression along the z axis, which coincides with an additional anisotropy axis along the direction of an external magnetic field. Such a composite feature of isofrequency surfaces (known as the *mixed-type* dispersion [49]) is conditioned by the hybrid character of Eq. (3) and appears when hyperbolicity in the permittivity tensor and gyrotropy in the permeability tensor exist simultaneously [21,49]. Moreover, from Figs. 3(a) and 3(b) one can conclude that the rotation symmetry of the isofrequency surfaces relative to the z axis is broken. The resulting form of isofrequency surfaces is typical for a biaxial crystal [22].

As the parameter δ_m increases, the ellipsoidlike surface is deformed gradually in such a way that its thickness decreases at the ellipsoid center and the surface transits to a toroid. Once the condition $|\mu_{xy}^2| = |\mu_{xx}\mu_{yy}|$ is fulfilled, the thickness of the ellipsoid at the center reduces to zero [Figs. 3(a) and 3(b)]. Subsequently, in the part of Region I where the condition $|\mu_{xy}^2| > |\mu_{xx}\mu_{yy}|$ holds, the isofrequency surface of the ordinary waves transits to a toroidlike form as shown in Fig. 2(c). Similar features have been recently reported for a hyperbolic-gyromagnetic metamaterial [21].

When both principal components ε_{zz} and μ_{xx} become negative quantities (Region II), there is a topological transition to a bihyperbolic topology for the isofrequency surface of the extraordinary waves. In this case there are two onefold type-II

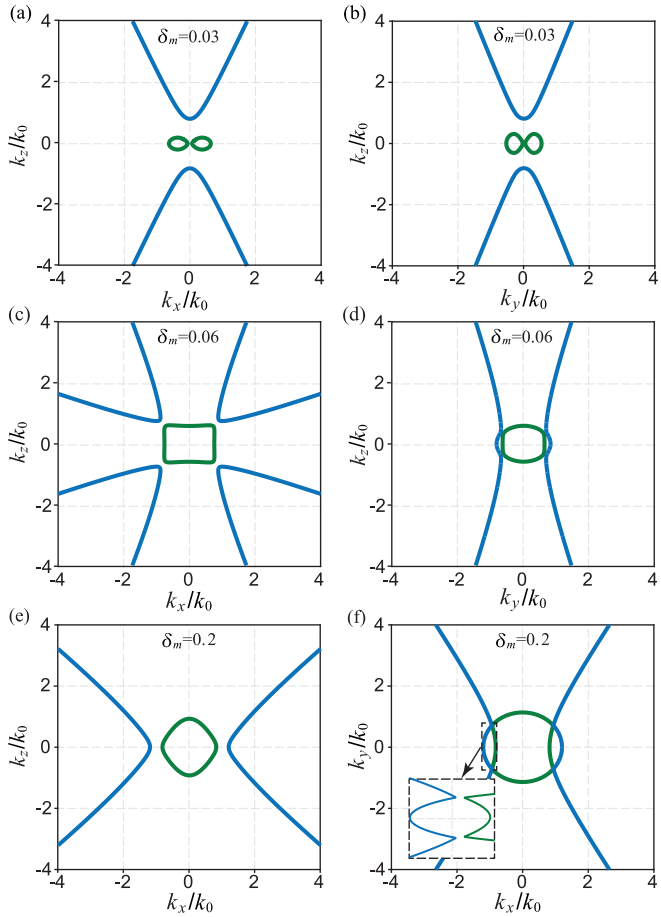

FIG. 3. The cross-section views of the isofrequency surfaces for different values of the parameter δ_m. The inset of panel (f) demonstrate disappearance of self-intersection points. Green and blue curves correspond to behaviors of ordinary and extraordinary waves, respectively.

hyperboloids with orthogonal revolution axes [Figs. 2(d), 2(e), and 3(c)]. Such an unusual bihyperbolic topology is a result of simultaneous effects of both the structure periodicity and an external magnetic field [33]. The isofrequency surface of the ordinary waves transits to an ellipsoidlike form since the condition $|\mu_{xy}^2| < |\mu_{xx}\mu_{yy}|$ is satisfied. This ellipsoid is surrounded by the bihyperbolic surface.

For the third set of parameters (Region III), all principal values of relative effective tensors are positive except for μ_{xx}. There is a topological transition of the isofrequency surface of the extraordinary waves to a type-I biaxial-hyperboloid oriented along the x axis [Fig. 2(f)]. As the parameter δ_m increases further, this surface gradually transits to a type-I uniaxial hyperboloid as shown in Fig. 2(g). In this case the isofrequency surfaces are strongly compressed along the z axis under the influence of an external static magnetic field. Another effect of this field is the absence of the degeneracy points (also known as *self-intersection* points [34]) in the isofrequency surfaces [Fig. 3(f)]. In turn, this means the disappearance of the conical refraction in anisotropic crystals [19,22] since the isofrequency surfaces split apart in these self-intersection points under an action of the external magnetic field [50,51].

Finally, in Region IV ($\delta_m \gg \delta_s$) all principal components of $\hat{\varepsilon}_{\text{eff}}$ and $\hat{\mu}_{\text{eff}}$ are positive quantities, the isofrequency surface is in the form of a single ellipsoid as shown in Fig. 2(h). In this region $\varepsilon_{xy} \to 0$, $\varepsilon_{xx} \approx \varepsilon_{yy} \approx \varepsilon_{zz} \to \varepsilon_m$, and the dispersion characteristic of a gyromagnetic (ferrite) bulk medium is dominant. For such a medium the topological transitions are well described (see, for instance, Ref. [20] and references therein).

IV. LOSS-INDUCED TOPOLOGICAL TRANSITIONS

The topological transitions and forms of isofrequency surfaces presented so far have been limited to the lossless case. However, if the operating frequency is close to the characteristic frequency of either ferromagnetic or plasma resonance, the intrinsic losses in constitutive materials of the superlattice are significant and thus cannot be ignored. In lossy media, components of the wave-vector $\vec{k}$ are complex quantities ($k_i = k_i' + ik_i''$, $i = x, y, z$, where k_i' represents the phase change and k_j'' corresponds to the decay rate), therefore losses may modify the forms of isofrequency surfaces [22,38,39]. These modifications are the subject of our further study. Of our prime interest are the conditions of occurrence of the loss-induced topological transitions of the isofrequency surfaces. To find these conditions, we again consider regions studied above for different δ_m's. To be specific, we have chosen the following values: $\delta_m = 0.02$, $\delta_m = 0.06$, and $\delta_m = 0.2$ which are representative values for Region I [Fig. 2(b)], Region II [Fig. 2(d)], and Region III [Fig. 2(f)], respectively. Since there are no peculiarities in Region IV, it is not considered in our further investigation.

In our model losses in magnetic and semiconductor layers are described by parameters b and ν, respectively (see the Appendix). Parameter b is the dimensionless one, whereas parameter ν has frequency units. For clarity, the dependence of both the real and the imaginary parts of the principal components of tensors $\hat{\mu}_{\text{eff}}$ and $\hat{\varepsilon}_{\text{eff}}$ on b and ν is shown in Fig. 4 for two values of δ_m.

When $\delta_m = 0.02$ (Region I) there are two combined conditions $0 < \mu_{xx}' < 1$ and $-1 < \varepsilon_{zz}' < 0$ on the real parts of the principal components of tensors $\hat{\mu}_{\text{eff}}$ and $\hat{\varepsilon}_{\text{eff}}$. Since μ_{xx}' is a small positive quantity, the superlattice behaves as a μ-near-zero medium, which features isofrequency surfaces in the form of an ellipsoid for ordinary waves and a type-I hyperboloid for extraordinary waves [Fig. 5(a)]. The revolution axis of the hyperboloid is oriented along the z axis.

Since losses are introduced to the system ($\nu \neq 0$ and $b \neq 0$, that is, $\mu_{ij}'' \neq 0$ and $\varepsilon_{ij}'' \neq 0$) the roots of Eq. (3) are now complex for both ordinary and extraordinary waves. Propagated waves decay exponentially, so they belong to the proper waves. Because of the wave attenuation in the system, the isofrequency surface of the extraordinary waves does not expand to infinity, and the type-I hyperboloid transforms to closed form [Fig. 5(b)]. The hyperbolic isofrequency surface of the extraordinary waves bends in the opposite direction at the finite value of $\vec{k}$ intersecting the ellipsoidlike isofrequency surface of the ordinary waves. In fact, a gradual increase in losses diminishes the size of the closed hyperboloidlike area and finally reduces it to zero. We should note that such loss-induced topological transitions of the isofrequency surface of

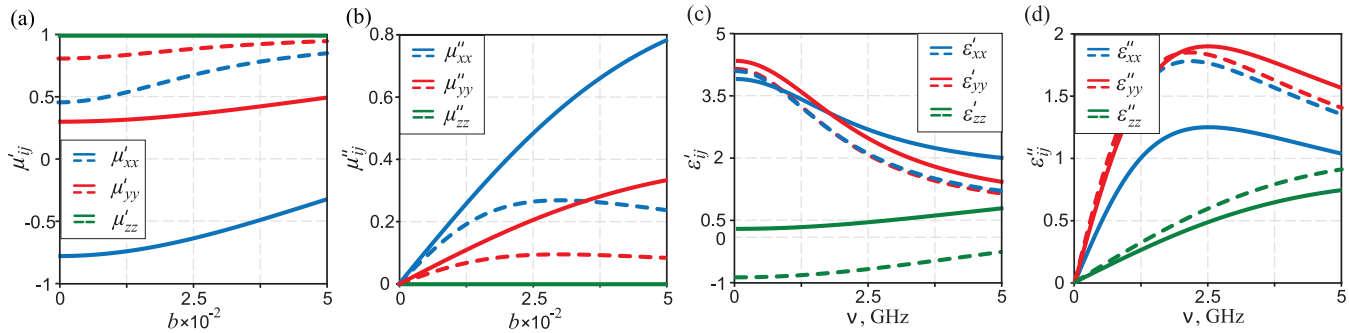

FIG. 4. (a) Real and imaginary parts of components of tensors, tensor $\hat{\mu}_{\text{eff}}$ as function of the dimensionless parameter b and (c) and (d) tensor $\hat{\varepsilon}_{\text{eff}}$ versus parameter ν given in gigahertz for two fixed values of δ_m. The dashed and solid lines correspond to $\delta_m = 0.02$ and $\delta_m = 0.2$, respectively. The other parameters are the same as in Fig. 1.

the extraordinary waves are quite usual for the hyperbolic metamaterials (see, for instance, Ref. [22]).

For the similar set of parameters and $\delta_m = 0.2$ (Region III), other conditions $-1 < \mu'_{xx} < 0$ and $0 < \varepsilon'_{zz} < 1$ are true. In this case the superlattice behaves as an ε-near-zero medium. For such a medium, loss-induced topological transitions, and forms of the isofrequency surfaces are similar to those described in the previous case. The sole exception is the revolution axis of the hyperboloid, which is now oriented along the x axis [Figs. 6(a) and 6(c)].

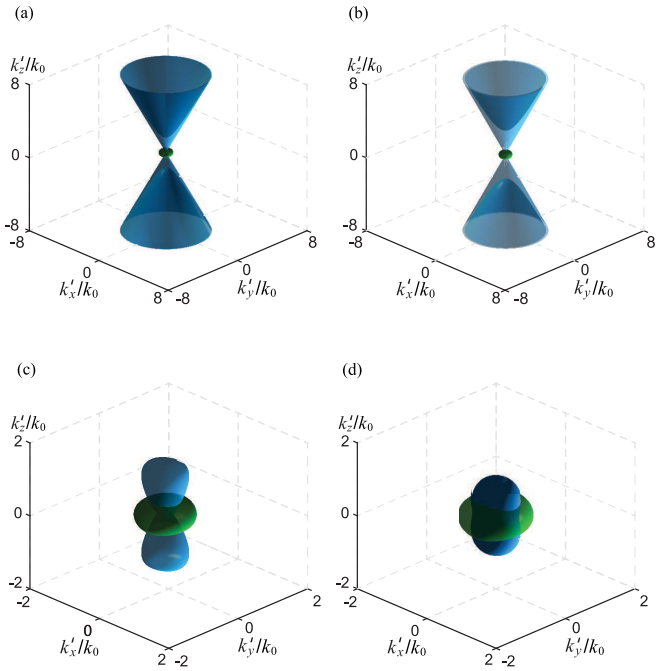

FIG. 5. The forms of isofrequency surfaces related to waves propagating through a superlattice characterized by different intrinsic losses inherent in actual magnetic and semiconductor materials. For these materials corresponding conditions $-1 < \varepsilon'_{zz} < 0$ and $0 < \mu'_{xx} < 1$ hold, and the value of $\delta_m = 0.02$ is assumed fixed. Parameters of the lossy system are as follows: (a) $b = 1 \times 10^{-4}$, $\nu = 1 \times 10^{-2}$ GHz; (b) $b = 5 \times 10^{-2}$, $\nu = 1 \times 10^{-2}$GHz; (c) $b = 1 \times 10^{-4}$, $\nu = 2$ GHz; (d) $b = 5 \times 10^{-2}$, $\nu = 2$ GHz. The green and blue surfaces are relative to ordinary and extraordinary waves, respectively.

Since the superlattice of interest consists of magnetic and semiconductor subsystems, these subsystems are both influenced by an external magnetic field. In this case the topological forms are distinct from those typical for traditional hyperbolic metamaterials. Indeed, when $\varepsilon'_{zz} < 0$ at a constant value of b, a nontrivial transition of the isofrequency surface of the extraordinary waves appears with an increase in ν. The size of the closed hyperboliclike area gradually decreases in the direction of the z axis, whereas it is expanded along both the x axis and the y axis. A complicated shape of the isofrequency surface of the extraordinary waves is conditioned by the loss-induced topological transitions from a type-I hyperboloid to a combination of two hyperboloids having orthogonal revolution axes. Therefore, with an increase in the losses in the semiconductor component, the corresponding hyperbolic

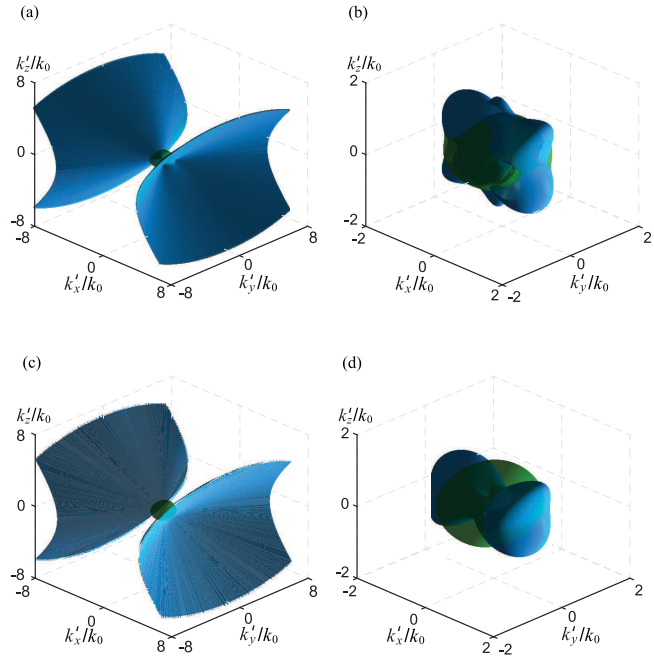

FIG. 6. The same as in Fig. 5 but for conditions $0 < \varepsilon'_{zz} < 1$, $-1 < \mu'_{xx} < 0$, and $\delta_m = 0.2$. Parameters of the lossy system are as follows: (a) $b = 1 \times 10^{-4}$, $\nu = 1 \times 10^{-2}$ GHz; (b) $b = 5 \times 10^{-2}$, $\nu = 1 \times 10^{-2}$ GHz; (c) $b = 1 \times 10^{-4}$, $\nu = 5$ GHz; (d) $b = 5 \times 10^{-2}$, $\nu = 5$ GHz.

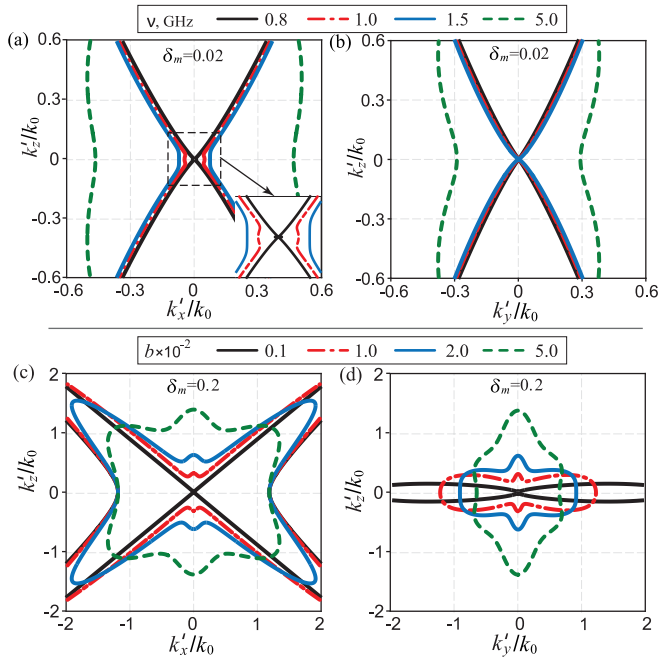

FIG. 7. The cross-section views of several stages of the loss-induced topological transitions of the isofrequency surface for the extraordinary waves; (a) and (b) $\delta_m = 0.02$ and $b = 2 \times 10^{-2}$; (c) and (d) $\delta_m = 0.2$ and $\nu = 1 \times 10^{-2}$ GHz.

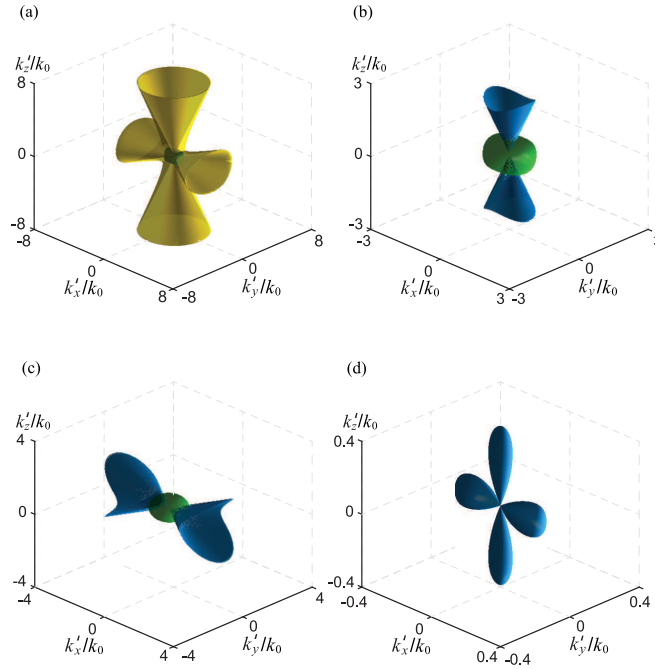

FIG. 8. The same as in Fig. 5 but for conditions $-1 < \varepsilon_{zz}' < 0$, $-1 < \mu_{xx}' < 0$, and $\delta_m = 0.06$. Parameters of the lossy material are as follows: (a) $b = 1 \times 10^{-4}$, $\nu = 1 \times 10^{-2}$ GHz; (b) $b = 1 \times 10^{-2}$, $\nu = 1 \times 10^{-2}$ GHz; (c) $b = 1 \times 10^{-4}$, $\nu = 2$ GHz; (d) $b = 2 \times 10^{-2}$, $\nu = 2$ GHz. The yellow surface corresponds to extraordinary improper waves, whereas the green and blue surfaces correspond to ordinary and extraordinary proper waves, respectively.

area becomes dominant, and the complicated bihyperboliclike shape appears [Figs. 5(c) and 5(d)].

When $\mu_{xx}' < 0$, ν is fixed, and b increases, the similar loss-induced transitions are observed in the superlattice with the dominant magnetic component [Fig. 6(b)]. In this case the closed isofrequency surface of the extraordinary wave undergoes compressing along both the x axis and the y axis and is expanded along the z axis. The variation of the closed area is accompanied by change in the shape of the isofrequency surface for the extraordinary waves [Figs. 6(b) and 6(d)]. We have added Fig. 7 to demonstrate peculiarities of these topological transitions which can be revealed from corresponding cross-section views calculated at particular values of δ_m (an animation of these transitions in the full range of parameters b and ν is available in the Supplemental Material [52]).

The most interesting is Region II where conditions $\mu_{xx}' < 0$ and $\varepsilon_{zz}' < 0$ for principal components of tensors $\hat{\mu}_{\text{eff}}$ and $\hat{\varepsilon}_{\text{eff}}$ hold. The superlattice behaves as an anisotropic double-negative and double-positive media for the extraordinary and ordinary waves, respectively. For the extraordinary waves the isofrequency surface appears in a form of bihyperboloid [33], which is significantly different from forms obtained above for Regions I and III [Fig. 8(a)].

Although such a form of the isofrequency surface is quite intriguing, it corresponds to the nonphysical solutions of Eq. (3) for small losses in the system. This means that the corresponding roots of Eq. (3) describe the propagation of the improper waves. In Fig. 8(a) we plot the isofrequency surface for the extraordinary improper waves with the yellow color.

The most complex effect is the competition between the losses in magnetic and semiconductor subsystems. It changes the propagation conditions for the extraordinary waves. Thus, under a certain level of either magnetic or semiconductor losses these waves become proper ones. In this case the isofrequency surface of the extraordinary waves acquires a loss-induced topological transition to a type-I hyperboloid with the revolution axis oriented either along the z axis [Fig. 8(b)] or the x axis [Fig. 8(c)] when either a magnetic ($\mu_{ij}'' \gg \varepsilon_{ij}''$) or a semiconductor ($\varepsilon_{ij}'' \gg \mu_{ij}''$) subsystem, respectively, is dominant (an animation of these loss-induced transitions can be found in the Supplemental Material [52]). Thus, one may conclude that in Region II the dispersion conditions of the extraordinary waves can be significantly modified (up to opposite conditions) by losses injected selectively into constitutive materials of the superlattice. Moreover, if there is no competition between the losses in subsystems, then the loss-induced bihyperboliclike topology arises [Fig. 8(d)].

V. CONCLUSIONS

We have studied the topological transitions of isofrequency surfaces in a biaxial gyroelectromagnetic medium influenced by an external static magnetic field. It has been demonstrated that in the case of a lossless structure the topological transitions from a closed ellipsoid to a bihyperboloid, or open type-I or type-II hyperboloids can be achieved. Such transitions of isofrequency surfaces occur at the critical points where principal components of the effective permeability and/or permittivity tensors change their sign.

The realization of the loss-induced topological transitions of the isofrequency surfaces was studied in detail. We have demonstrated that several distinctive loss-induced topological transitions of the isofrequency surface of the extraordinary waves can be achieved by providing selective injection of losses into magnetic and semiconductor subsystems of the superlattice. It has been revealed that the loss-induced topological transition from a type-I hyperboloid to a bihyperboloid occurs when the real part of the principal component of permittivity and/or permeability is close to zero, whereas its imaginary part is high.

ACKNOWLEDGMENT

The authors acknowledge Jilin University's hospitality and financial support and useful discussions and collaboration with V. I. Shcherbinin.

APPENDIX: CONSTITUTIVE PARAMETERS OF FERRITE AND SEMICONDUCTOR LAYERS

The expressions for the tensors' components of the underlying constitutive parameters of magnetic $\hat{\mu}_m \to \hat{g}_m$ and semiconductor $\hat{\varepsilon}_s \to \hat{g}_s$ layers can be written in the form

$$\hat{g}_j = \begin{pmatrix} g_1 & ig_2 & 0 \\ -ig_2 & g_1 & 0 \\ 0 & 0 & g_3 \end{pmatrix}. \tag{A1}$$

For magnetic layers [53,54] the components of tensor $\hat{g}_m$ are $g_1 = 1 + \chi' + i\chi''$, $g_2 = \Omega' + i\Omega''$, $g_3 = 1$, and $\chi' = \omega_0\omega_m[\omega_0^2 - \omega^2(1-b^2)]D^{-1}$, $\chi'' = \omega\omega_m b[\omega_0^2 + \omega^2(1+b^2)]D^{-1}$, $\Omega' = \omega\omega_m[\omega_0^2 - \omega^2(1+b^2)]D^{-1}$, $\Omega'' = 2\omega^2\omega_0\omega_m bD^{-1}$, $D = [\omega_0^2 - \omega^2(1+b^2)]^2 + 4\omega_0^2\omega^2 b^2$, where ω_0 is the Larmor frequency and b is the dimensionless damping constant.

For semiconductor layers [55] the components of tensor $\hat{g}_s$ are $g_1 = \varepsilon_l[1 - \omega_p^2(\omega + i\nu)\{\omega[(\omega + i\nu)^2 - \omega_c^2]\}^{-1}]$, $g_2 = \varepsilon_l\omega_p^2\omega_c\{\omega[(\omega + i\nu)^2 - \omega_c^2]\}^{-1}$, $g_3 = \varepsilon_l\{1 - \omega_p^2[\omega(\omega + i\nu)]^{-1}\}$, where ε_l is the part of the permittivity of the lattice, ω_p is the plasma frequency, ω_c is the cyclotron frequency, and ν is the electron collision frequency in plasma.

Relative permittivity ε_m of the ferrite layers as well as relative permeability μ_s of the semiconductor layers are scalar quantities.

[1] L. Ferrari, C. Wu, D. Lepage, X. Zhang, and Z. Liu, Prog. Quantum Electron. **40**, 1 (2015).
[2] C. L. Cortes, W. Newman, S. Molesky, and Z. Jacob, J. Opt. **14**, 063001 (2012).
[3] A. N. Poddubny, P. A. Belov, and Y. S. Kivshar, Phys. Rev. B **87**, 035136 (2013).
[4] Z. Jacob, I. I. Smolyaninov, and E. E. Narimanov, Appl. Phys. Lett. **100**, 181105 (2012).
[5] Z. Liu, H. Lee, Y. Xiong, C. Sun, and X. Zhang, Science **315**, 1686 (2007).
[6] D. R. Smith, D. Schurig, J. J. Mock, P. Kolinko, and P. Rye, Appl. Phys. Lett. **84**, 2244 (2004).
[7] P. V. Kapitanova, P. Ginzburg, F. J. Rodríguez-Fortuño, D. S. Filonov, P. M. Voroshilov, P. A. Belov, A. N. Poddubny, Y. S. Kivshar, G. A. Wurtz, and A. V. Zayats, Nat. Commun. **5**, 3226 (2014).
[8] D. R. Smith and D. Schurig, Phys. Rev. Lett. **90**, 077405 (2003).
[9] J. Schilling, Phys. Rev. E **74**, 046618 (2006).
[10] S. V. Zhukovsky, O. Kidwai, and J. E. Sipe, Opt. Express **21**, 14982 (2013).
[11] A. Poddubny, I. Iorsh, P. Belov, and Y. Kivshar, Nat. Photonics **7**, 948 (2013).
[12] C. R. Simovski, P. A. Belov, A. V. Atrashchenko, and Y. S. Kivshar, Adv. Mater. **24**, 4229 (2012).
[13] J. Sun, J. Zeng, and N. M. Litchinitser, Opt. Express **21**, 14975 (2013).
[14] M. S. Mirmoosa, S. Y. Kosulnikov, and C. R. Simovski, Phys. Rev. B **92**, 075139 (2015).
[15] M. S. Mirmoosa, S. Y. Kosulnikov, and C. R. Simovski, Phys. Rev. B **94**, 075138 (2016).
[16] O. Kidwai, S. V. Zhukovsky, and J. E. Sipe, Phys. Rev. A **85**, 053842 (2012).
[17] J. B. Pendry, A. J. Holden, D. J. Robbins, and W. J. Stewart, IEEE Trans. Microwave Theory Tech. **47**, 2075 (1999).
[18] R. K. Fisher and R. W. Gould, Phys. Rev. Lett. **22**, 1093 (1969).
[19] E. V. Kuznetsov and A. M. Merzlikin, Opt. Commun. **405**, 164 (2017).
[20] E. G. Lokk, J. Commun. Technol. Electron. **62**, 251 (2017).
[21] R.-L. Chern and Y.-Z. Yu, Opt. Express **25**, 11801 (2017).
[22] K. E. Ballantine, J. F. Donegan, and P. R. Eastham, Phys. Rev. A **90**, 013803 (2014).
[23] M. I. Kaganov, N. B. Pustyl'nik, and T. I. Shalaeva, Phys. Usp. **40**, 181 (1997).
[24] R.-X. Wu, T. Zhao, and J. Q. Xiao, J. Phys.: Condens. Matter **19**, 026211 (2007).
[25] R. H. Tarkhanyan and D. G. Niarchos, Phys. Status Solidi B **245**, 154 (2008).
[26] O. V. Shramkova, Prog. Electromagn. Res. M **7**, 71 (2009).
[27] R. Tarkhanyan, D. Niarchos, and M. Kafesaki, J. Magn. Magn. Mater. **322**, 603 (2010).
[28] V. R. Tuz and V. I. Fesenko, in *Contemporary Optoelectronics*, edited by O. Shulika and I. Sukhoivanov, Springer Series in Optical Sciences Vol. 199 (Springer, Dordrecht, The Netherlands, 2016), pp. 99–113.
[29] V. R. Tuz, J. Magn. Magn. Mater. **419**, 559 (2016).
[30] V. I. Fesenko, I. V. Fedorin, and V. R. Tuz, Opt. Lett. **41**, 2093 (2016).
[31] V. R. Tuz, V. I. Fesenko, I. V. Fedorin, H.-B. Sun, and W. Han, J. Appl. Phys. **121**, 103102 (2017).
[32] V. R. Tuz, V. I. Fesenko, I. V. Fedorin, H.-B. Sun, and V. M. Shulga, Superlattice. Microst. **103**, 285 (2017).
[33] V. R. Tuz, I. V. Fedorin, and V. I. Fesenko, Opt. Lett. **42**, 4561 (2017).
[34] L. D. Landau and E. M. Lifshitz, *Electrodynamics of Continuous Media (Volume 8 of A Course of Theoretical Physics)* (Pergamon, Oxford, 1960).
[35] L. B. Felsen and N. Marcuvitz, *Radiation and Scattering of Waves* (IEEE-Wiley, New York, 1994).

[36] S. Feng, Phys. Rev. Lett. **108**, 193904 (2012).
[37] H. Jiang, W. Liu, K. Yu, K. Fang, Y. Sun, Y. Li, and H. Chen, Phys. Rev. B **91**, 045302 (2015).
[38] K. Yu, Z. Guo, H. Jiang, and H. Chen, J. Appl. Phys. **119**, 203102 (2016).
[39] Z. Guo, H. Jiang, Y. Sun, Y. Li, and H. Chen, Appl. Sci. **8**, 596 (2018).
[40] V. Agranovich, Solid State Commun. **78**, 747 (1991).
[41] V. R. Tuz, O. D. Batrakov, and Y. Zheng, Prog. Electromagn. Res. B **41**, 397 (2012).
[42] V. R. Tuz, J. Opt. **17**, 035611 (2015).
[43] V. R. Tuz, I. V. Fedorin, and V. I. Fesenko, in *Surface Waves*, edited by F. Ebrahimi (IntechOpen, Rijeka, 2018), Chap. 6.
[44] T. Mulkey, J. Dillies, and M. Durach, Opt. Lett. **43**, 1226 (2018).
[45] A. Ishimaru, *Electromagnetic Wave Propagation, Radiation, and Scattering* (Prentice Hall, Englewood Cliffs, NJ, 1991).
[46] P. Yu, V. I. Fesenko, and V. R. Tuz, Nanophotonics **7**, 925 (2018).
[47] R. X. Wu, J. Appl. Phys. **97**, 076105 (2005).
[48] S. M. Sze and J. C. Irvin, Solid-State Electron. **11**, 599 (1968).
[49] P.-H. Chang, C.-Y. Kuo, and R.-L. Chern, Opt. Express **22**, 25710 (2014).
[50] A. G. Khatkevich and S. N. Kurilkina, J. Appl. Spectrosc. **51**, 1329 (1989).
[51] A. Belsky and M. Stepanov, Opt. Commun. **204**, 1 (2002).
[52] See Supplemental Material at http://link.aps.org/supplemental/10.1103/PhysRevB.99.094404 for visualization of the loss-induced topological transitions of isofrequency surfaces related to Figs. 5, 6, and 8 of the paper.
[53] A. G. Gurevich, *Ferrites at Microwave Frequencies* (Heywood, London, 1963).
[54] R. E. Collin, *Foundation for Microwave Engineering* (Wiley-Interscience, New York, 1992).
[55] F. Bass and A. Bulgakov, *Kinetic and Electrodynamic Phenomena in Classical and Quantum Semiconductor Superlattices* (Nova Science, Hauppauge, NY, 1997).